DOI: 10.1002/zaac.201200511

Na_3SbS_3: Single Crystal X-ray Diffraction, Raman Spectroscopy, and Impedance Measurements

Constantin Pompe[a] and Arno Pfitzner*[a]

Dedicated to Professor Hartmut Bärnighausen on the Occasion of His 80th Birthday

Keywords: Chalcogenometalates; Sodium; Ion conductor; Crystal structure; Raman spectroscopy

Abstract. Na_3SbS_3 was prepared by the reaction of anhydrous Na_2S, antimony, and sulfur in a ratio of 3:2:3 at 870 K. The pale yellow compound is air and moisture sensitive. A microcrystalline sample was obtained after annealing Na_3SbS_3 for two weeks at 720 K. The crystal structure of Na_3SbS_3 was determined by single-crystal X-ray diffraction at 123 K. Na_3SbS_3 crystallizes in the cubic space group $P2_13$ (No. 198) with a = 8.6420(1) Å, V = 645.42(1) Å^3 and Z = 4. The structure refinement converged to R = 0.0099 (wR = 0.0181) for 592 independent reflections and 23 parameters. Na_3SbS_3 is isotypic with Na_3AsS_3. Sodium atoms are located on three different sites, which show a strongly distorted octahedral coordination sphere of sulfur. The coordination polyhedra of equivalent sodium sites share common vertices, whereas those of different sodium sites share common faces. Antimony and sulfur form trigonal SbS_3 pyramids, which coordinate sodium as a mono-, bi-, or tridentate ligand. Raman spectroscopic investigations result in stretching modes ν(Sb–S) at 334, 321, and 312 cm^{-1}, respectively. Thermoanalytical studies do not show any additional thermal effects up to the melting point of 875 K. Impedance spectroscopy on Na_3SbS_3 in a range from 325 to 570 K shows a temperature dependent Na^+ conductivity, which is 1.9×10^{-6} Ω^{-1}·cm^{-1} at 570 K.

Introduction

Alkali metal pnicogen chalcogenides M_3PnQ_3 (M = Na, K, Rb, Cs, Pn = As, Sb, Bi, and Q = S, Se, Te) are a well-established group of compounds. Although the homologous elements differ significantly from each other in terms of ion radii and electronegativity, they form a whole series of isotypic crystal structures, and crystallize in the cubic space group $P2_13$. The structure type is named after the first representative Na_3AsS_3.[1] *Sommer* and *Hoppe* as well as *Bronger* et al. had a great merit on the synthesis and structural characterization of the corresponding compounds. *Sommer* described the sodium and potassium containing thioarsenates (Na_3AsS_3, K_3AsS_3,) and thioantimonates (Na_3SbS_3, K_3SbS_3),[2] whereas *Bronger* and co-workers focused on the selenoarsenates (Na_3AsSe_3, K_3AsSe_3), selenoantimonates (K_3SbSe_3, Rb_3SbSe_3, Cs_3SbSe_3), and the selenobismutates (K_3BiSe_3, Rb_3BiSe_3, Cs_3BiSe_3).[3–6] The telluroantimonates Na_3SbTe_3 and K_3SbTe_3 were also reported in literature.[7,8] *Jung* firstly investigated the conductivity of a compound of this series M_3PnQ_3, i.e., K_3SbTe_3, which was reported to be a poor semiconductor.[9] Very recently the thioantimonate Li_3SbS_3 was structurally characterized. It is the first member of this whole group of materials, which crystallizes in a different structure type. It shows an ionic conductivity of 5.4×10^{-5} Ω^{-1}·cm^{-1}.[10] In contrary, Na_3SbSe_3 crystallizes in the well-established Na_3AsS_3 structure type and shows also an enhanced ionic conductivity at elevated temperature.[11]

Herein, we report on the structural characterization and the ionic conductivity of the corresponding thioantimonate, Na_3SbS_3. To date, only lattice parameters are known, which are based on Guinier powder data, and isotypism to Na_3AsS_3 has been proposed.[2]

Results and Discussion

Structure Description and Discussion

The crystal structure of Na_3SbS_3 was determined from single-crystal X-ray diffraction data collected at 123 K. The title compound crystallizes in space group $P2_13$. The cubic cell has the parameters a = 8.6420(1) Å, V = 645.42(1) Å^3 and Z = 4. From powder diffraction data of pure powder samples a cell parameter of a = 8.7026(5) Å was determined at room temperature. Crystallographic data are listed in Table 1. The structure refinement with anisotropic displacement parameters converged to R_1 = 0.0099 [23 parameters, 592 reflections with $I > 2\sigma(I)$] and wR_2 = 0.0181 (all reflections). Atomic coordinates and equivalent isotropic displacement parameters U_{eq} are listed in Table 2, the anisotropic displacement parameters U_{ij} in Table 3.

The Na_3AsS_3 structure type and its relations to the $NaClO_3$ as well as to the Th_3P_4 structure type has already been discussed in several publications.[2,6] Thus, we limit the dis-

* Prof. Dr. A. Pfitzner
Fax: +49-941-943-814551
E-Mail: arno.pfitzner@chemie.uni-regensburg.de
[a] Institut für Anorganische Chemie
Universität Regensburg
Universitätsstraße 31
93040 Regensburg, Germany

Zeitschrift für anorganische und allgemeine Chemie ZAAC Journal of Inorganic and General Chemistry

Table 1. Crystallographic data for the structure analysis of Na_3SbS_3.

	Na_3SbS_3
Formula weight /g·mol^{-1}	286.90
Color	pale yellow
Crystal system	cubic
Space group	$P2_13$ (No. 198)
Lattice constant a /Å	8.6420(1)
Cell volume V /Å^3	645.42(1)
Number of formula units per unit cell Z	4
Calculated density ρ_{calc} /g·cm^{-3}	2.953
Temperature T /K	123
Wavelength λ /Å	0.71073
Diffractometer	Oxford Diffraction Gemini R Ultra CCD, Mo-K_α (λ = 0.71073 Å)
Absorption coeff. μ /mm^{-1}	5.308
Absorption correction	Multi-scan[19]
2θ range /°	$6.66 \leq 2\theta \leq 58.68$
hkl-ranges	$-11 \leq h \leq 10$ $-11 \leq k \leq 10$ $-11 \leq l \leq 11$
No. of reflections, R_{int}	9385, 0.0337
No. of independent reflections	592
Structure solution	SIR92[20]
Structure refinement	SHELX-97[21]
No. of parameters	23
Final R, wR [$I > 2\sigma(I)$]	0.0099, 0.0180
Final R, wR (all reflections)	0.0106, 0.0181
GooF	1.099
Largest difference peak $\Delta\rho_{max}$ and hole $\Delta\rho_{min}$ /e·Å^{-3}	0.451, -0.264
Extinction parameter	0.0016(2)
Flack parameter	–0.04(2)

Table 2. Atomic coordinates and equivalent isotropic displacement parameters U_{eq}[a)] for Na_3SbS_3.

Atom	Wyck.	x	y	z	U_{eq}
Na1	4*a*	0.82507(8)	x	x	0.0167(3)
Na2	4*a*	0.56826(8)	x	x	0.0117(3)
Na3	4*a*	0.05968(8)	x	x	0.0119(3)
Sb	4*a*	0.28492(1)	x	x	0.00775(6)
S	12*b*	0.01647(5)	0.24997(4)	0.35818(5)	0.01027(9)

a) U_{eq} is defined as one third of the trace of the orthogonalized U_{ij} tensor.

Table 3. Anisotropic displacement parameters U_{ij} for Na_3SbS_3.

Atom	U_{11}	U_{22}	U_{33}	U_{23}	U_{13}	U_{12}
Na1	0.0167(3)	U_{11}	U_{11}	0.0005(3)	U_{23}	U_{23}
Na2	0.0117(3)	U_{11}	U_{11}	0.0005(3)	U_{23}	U_{23}
Na3	0.0119(3)	U_{11}	U_{11}	–0.0003(3)	U_{23}	U_{23}
Sb	0.00775(6)	U_{11}	U_{11}	–0.00044(4)	U_{23}	U_{23}
S	0.0092(2)	0.0101(2)	0.0116(2)	0.0005(2)	0.0025(2)	0.0005(2)

cussion herein to the most important details. Distances and angles are based on the data obtained at 123 K.

The crystal structure of Na_3SbS_3 can be subdivided into two structural motifs. Antimony and sulfur are arranged as trigonal-pyramidal SbS_3 units (see Figure 2) with an angle S–Sb–S = 99.40(1)°, the distance d(Sb–S) is 2.4237(4) Å. So-called secondary bonds are formed to three sulfur atoms at a distance of 3.6890 Å. A detailed comparison with isotypic thioantimonates(III) of the other alkali metals is not possible due to a lack of precise structural data for some of them. However, Li_3SbS_3 was synthesized recently.[10] It represents a completely different structure type as compared with the other compounds of the series M_3PnQ_3. Nevertheless, the SbS_3 units therein show the typical bond lengths and angles, regardless the fact that they do not have perfect trigonal symmetry in Li_3SbS_3. The trigonal-pyramidal SbS_3 motif was also found in compounds like Cu_3SbS_3, $(CuI)_2Cu_3SbS_3$, or $(AgI)_2Ag_3SbS_3$. The distance Sb–S in Cu_3SbS_3 varies between 2.446 and 2.478 Å.[12] Shorter distances were observed in $(CuI)_2Cu_3SbS_3$ (2.434 to 2.446 Å).[13] In silver containing analogue $(AgI)_2Ag_3SbS_3$, the distances range from 2.418 to 2.426 Å at 173 K.[14]

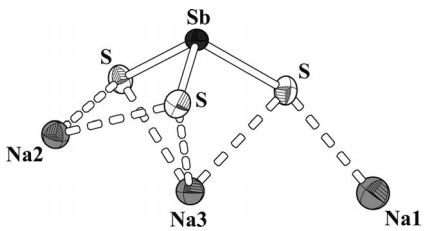

Figure 2. Coordination of antimony in the SbS_3 units and sodium in the next coordination sphere.

Figure 1 shows the three different coordination modes of SbS_3 units to the three different sodium sites Na1, Na2, and

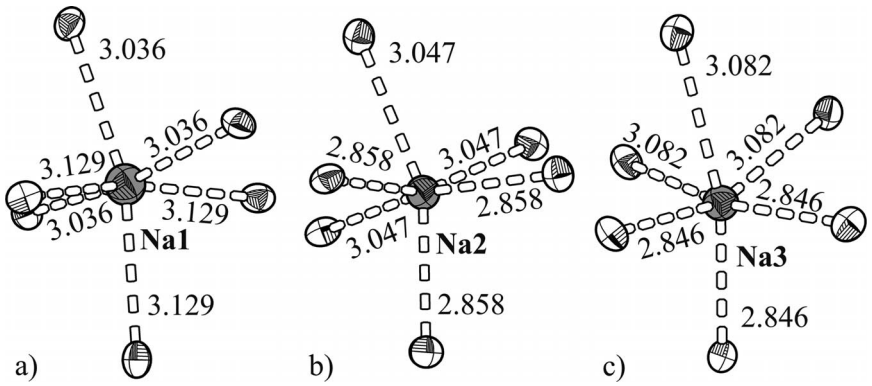

Figure 1. The distorted octahedral coordination of the three sodium sites Na1 (a), Na2 (b), and Na3 (c). Distances are given in Å.

Na3 in Na_3SbS_3. Na1 is coordinated exclusively by monodentate and Na2 by bidentate SbS_3 ligands, respectively. Na3 is coordinated by one tridentate as well as by three monodentate ligands. These coordination modes result in three different distorted octahedral environments for the sodium atoms. The interatomic distances in Table 4 quantify the distortions of the NaS_6 units. Several examples of SbS_3 units acting as bidentate ligands to transition metals in competition with ammines have been recently reported.[15–18] However, in these examples only one coordination mode is observed.

Table 4. Selected interatomic distances /Å and angles /° for Na_3SbS_3 at 123 K.

Sb–S	3×	2.4237(4)	S–Sb–S	3×	99.40(1)
	3×	3.6890(4)			
Na1–S	3×	3.0355(9)	S–Na1–S	3×	83.65(3)
	3×	3.1288(9)	S–Na1–S	3×	84.49(3)
			S–Na1–S	3×	86.79(1)
			S–Na1–S	3×	107.385(7)
			S–Na1–S	3×	164.53(1)
Na2–S	3×	2.8580(7)	S–Na2–S	3×	77.46(2)
	3×	3.0465(9)	S–Na2–S	3×	84.12(3)
			S–Na2–S	3×	95.63(3)
			S–Na2–S	3×	105.998(7)
			S–Na2–S	3×	157.76(2)
Na3–S	3×	2.8461(8)	S–Na3–S	3×	73.71(3)
	3×	3.082(1)	S–Na3–S	3×	86.93(2)
			S–Na3–S	3×	94.29(3)
			S–Na3–S	3×	105.368(8)
			S–Na3–S	3×	160.17(3)

The distances d(Na–S) in Na_3SbS_3 vary between 2.846 and 3.129 Å. A calculated distance of d_{calc}(Na–S) = 2.86 Å results from ionic radii.[22] Typically compounds adopting the Na_3AsS_3 structure type show two alkali metal sites with bond lengths in the range of those calculated from ionic radii and one with significantly longer distances to coordinating chalcogen atoms.[11] This is also the case in the title compound with the longer distances observed for Na1, compare Table 4.

Powder X-ray Diffraction

In Figure 3 the pattern, calculated from single crystal structural data, is opposed as inverted intensities to the experimental pattern. A high background in the experimental pattern is due to the measurement in a sealed glass capillary. The comparison between both patterns indicates the purity of the sample, which was subsequently used for impedance measurements. The refined cell constant a = 8.7026(5) Å matches the value, which was presented by *Sommer* and *Hoppe*.[2]

Raman Spectroscopy

The bonding interactions between antimony and sulfur can be estimated by the resonance of the Sb–S stretching vibrations of the SbS_3 units.[13] In case of Na_3SbS_3 they lead to dominating bands in the range between 334 and 312 cm^{-1} (see Figure 4). The values agree quite well with the spectra for related compounds like Li_3SbS_3 (333–301 cm^{-1}) or Ag_3SbS_3 (330–303 cm^{-1}).[10,14] Therein SbS_3 pyramids are not completely isolated from each other, which means corresponding distances $d_{secondary}$(Sb–S) are about 3.7 Å. In this case the secondary bonding interactions between the SbS_3 units and the next-nearest sulfur atoms cause a typical red shift in comparison to compounds, in which the SbS_3 units are separated from each other. $(AgI)_2Ag_3SbS_3$ e.g., shows resonances between 357 and 316 cm^{-1}.[14]

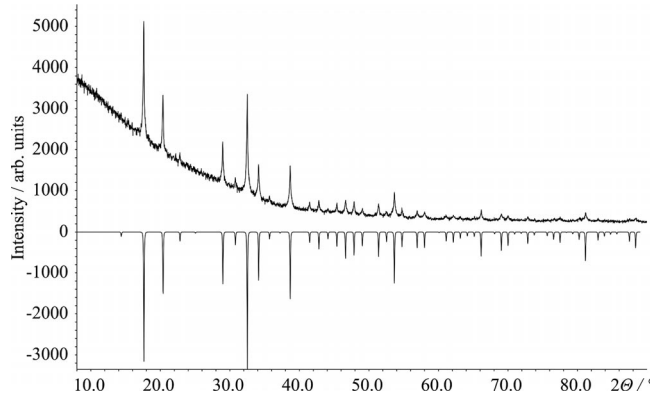

Figure 3. The measured (top) and calculated X-ray powder diffraction pattern for Na_3SbS_3 (down, inverted intensities). All measured lines can be indexed with a cubic primitive cell with a = 8.7026(5) Å.

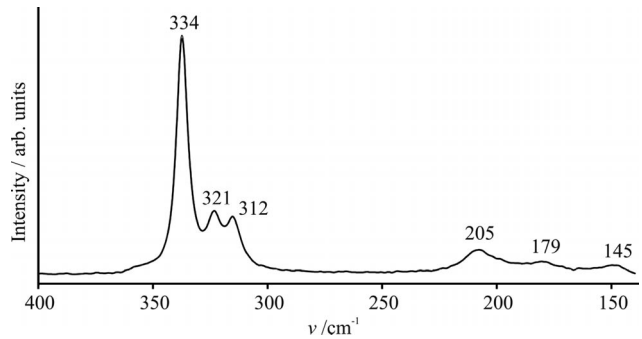

Figure 4. The Raman spectrum shows the bands of the of the Sb–S stretching modes at 334, 321, and 312 cm^{-1}.

Differential Thermal Analysis (DTA)

A pure, finely powdered sample of Na_3SbS_3 was used for DTA. The melting and the crystallization curves show one maximum, respectively. The melting point of Na_3SbS_3 is observed at 876 K. The compound crystallizes at 724 K. Similar dystectic behavior was reported for the selenide analogue Na_3SbSe_3.[11] An additional endothermic effect was reported for heating curves of Na_3SbS_3 and a high-temperature modification was suggested in reference [23] without further characterization. Further experiments, e.g., high-temperature X-ray diffraction will clarify this inconsistency.

Zeitschrift für anorganische und allgemeine Chemie ZAAC Journal of Inorganic and General Chemistry

Impedance Measurement

For the determination of the total electric conductivity of Na_3SbS_3 frequency dependent impedance spectroscopy was performed in a temperature range from 325 to 570 K. The Nyquist plot in Figure 5 shows the relation between the real and imaginary part of the impedance at 570 K. The linear arc for frequencies below 1 kHz is generated by ionic conductivity, which increases from $1 \times 10^{-9}\ \Omega^{-1}\cdot cm^{-1}$ at 325 K to $2 \times 10^{-6}\ \Omega^{-1}\cdot cm^{-1}$ at 570 K.

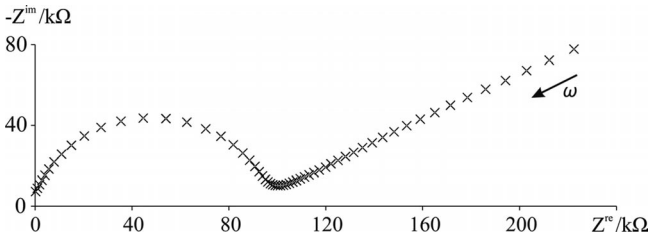

Figure 5. Impedance spectrum of Na_3SbS_3 at 570 K. The spectrum shows the typical frequency dependency in case of an ionic conductor with ion blocking electrodes.

The dependency of ionic conductivity on temperature is illustrated by the Arrhenius plot in Figure 6. The activation energy is 0.49 eV. The presented results for Na_3SbS_3 differ in some case from the recently published values for Na_3SbSe_3. The ionic conductivity of the selenide compound reaches a slightly higher value ($3 \times 10^{-6}\ \Omega^{-1}\cdot cm^{-1}$ at 570 K).[11] The conductivities of both sodium antimony chalcogenides are well comparable for example to sodium tetrathiophosphate, which shows an ionic conductivity of $4 \times 10^{-6}\ \Omega^{-1}\cdot cm^{-1}$ at 323 K.[24] However, Na_3SbSe_3 shows a significant higher activation energy of 0.69 eV than Na_3SbS_3. Ionic conductivity was not detectable below 380 K. *Jansen* reported decreasing activation energies of the low-temperature modification for the series $Na_3PO_4S_{4-x}$ (x = 0, 1, 2, 3, 4). This observation is explained by the increasing polarisability of the anion lattice from Na_3PO_4 to Na_3PS_4.[25] Another example for this trend are the silver ion conducting compounds $Ag_5Te_{2-y}Se_yCl$ (y = 0–0.7), whose activation energies decrease with an increasing content of tellurium.[26] Our studies on Na_3SbS_3 and Na_3SbSe_3 result in a contrary tendency so far. Therefore further investigations on compounds with a mixed chalcogenide lattice are in progress.

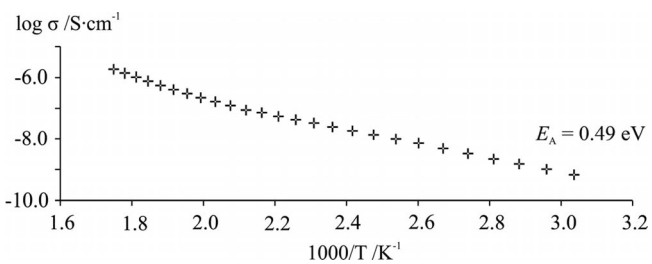

Figure 6. The Arrhenius plot shows an exponential dependency of the specific ionic conductivity on the reciprocal temperature.

Experimental Section

Synthesis: Pure samples of Na_3SbS_3 for X-ray powder diffraction and impedance spectroscopy were obtained from stoichiometric mixtures of Na_2S, antimony (99.9999 %, Chempur) and sulfur (99.999 %, Chempur) in a 3:2:3 ratio, which were heated to 870 K in evacuated silica ampoules for 7 d. The ampoules were coated with graphite by pyrolysis of acetone prior to use. Anhydrous Na_2S was obtained by reaction of stoichiometric quantities of distilled sodium (99 %, Merck) and sulfur in dry ammonia.[27] Due to their air and moisture sensitivity, all procedures with Na_2S and Na_3SbS_3 were performed in an atmosphere of dry argon. For the structure determination of Na_3SbS_3, pale yellow single crystals were obtained after a second annealing period of two weeks at 720 K.

Crystal Structure Analysis: A transparent, pale yellow single crystal of Na_3SbS_3 was measured in a drop of mineral oil. A nitrogen jet cooled the sample down to 123 K in order to fix the crystal during the data collection. Diffraction data were collected with an Oxford Diffraction Gemini R Ultra CCD with Mo-K_α radiation (λ = 0.71073 Å). Absorption correction was carried out by multi-scans.[19] The crystal structure was solved by direct methods with SIR92.[20] SHELX-97 was used for full-matrix least-squares structure refinement, applying anisotropic displacement parameters for all atoms.[21] An extinction parameter was introduced in the final stage of the refinement. The Flack parameter of almost 0 did not indicate any inversion twinning.

Powder X-ray Diffraction: Finely ground samples were sealed in an argon atmosphere in a glass capillary (diameter 0.2 mm). X-ray powder patterns were measured with a STOE Stadi P diffractometer with monochromatic Cu-$K_{\alpha1}$ radiation (λ = 1.540598 Å) and a Ge-monochromator at room temperature. The intensities were collected in a 2θ range from 8.0° to 90° and evaluated with the STOE program package WINXPOW.[28]

Further details of the crystal structure investigations may be obtained from the Fachinformationszentrum Karlsruhe, 76344 Eggenstein-Leopoldshafen, Germany (Fax: +49-7247-808-666; E-Mail: crysdata@fiz-karlsruhe.de, http://www.fiz-karlsruhe.de/request for deposited data.html) on quoting the depository number CSD-425458.

Raman Spectroscopy: Raman spectra were recorded with a Varian FTS 7000e Spectrometer with a Nd:YAG laser (λ = 1064 nm) and a germanium detector cooled by liquid nitrogen. Samples were sealed in glass capillaries (diameter 0.5 mm) and measured in back-scattering mode. The signals were Fourier transformed by a Varian FT-Raman module and analyzed with the software Varian resolutions pro.[29]

Differential Thermal Analysis: The thermal behavior was recorded with a Setaram DTA-TG 92–16.18. A small amount of the powdered sample was filled in a capillary tube (diameter 1.5 mm) and sealed under vacuum. The tube was heated up from 298 to 1073 K and cooled down again to room temperature with a heating/cooling rate of 10 $K\cdot min^{-1}$. Onset temperatures of the melting and crystallization process are derived from the respective curves.

Impedance Spectroscopy: Frequency dependent impedance spectroscopy of Na_3SbS_3 was carried out with an experimental set-up described earlier in a silica tube in an atmosphere of dry argon.[30] The heating cycles proceeded in a temperature range from 325 to 570 K in steps of 10 K. During a measurement the applied frequency was raised from 1 Hz to 1 MHz with an IMd6A from Zahner Elektrik. Data were collected and analyzed with the software Thales Flink.[31] Na_3SbS_3

was cold pressed (20 min, 7000 kg·cm^{-2}) to a pellet with 93 % of the calculated density. It was inserted in the spring-loaded conductivity jig according to the scheme Pt|Au|Na_3SbS_3|Au|Pt, where gold acts as ion blocking electrode.

Acknowledgements

We thank *Dr. M. Bodensteiner* for collecting single-crystal X-ray diffraction data and *Prof. Dr. N. Korber* for providing the ammonia condensation plant.

References

[1] M. Palazzi, *Acta Crystallogr., Sect. B Struct. Sci.* **1976**, *32*, 3175.
[2] H. Sommer, R. Hoppe, *Z. Anorg. Allg. Chem.* **1977**, *430*, 199.
[3] W. Bronger, A. Donike, D. Schmitz, *Z. Anorg. Allg. Chem.* **1998**, *624*, 553.
[4] W. Bronger, A. Donike, D. Schmitz, *Z. Anorg. Allg. Chem.* **1999**, *625*, 435.
[5] W. Bronger, A. Donike, D. Schmitz, *Z. Anorg. Allg. Chem.* **1996**, *622*, 1003.
[6] W. Bronger, A. Donike, D. Schmitz, *Z. Anorg. Allg. Chem.* **1997**, *623*, 1715.
[7] J. Lin, G. J. Miller, *J. Solid State Chem.* **1994**, *113*, 296.
[8] B. Eisenmann, R. Zagler, *Z. Kristallogr.* **1991**, *197*, 255.
[9] J.-S. Jung, B. Wu, E. D. Stevens, C. J. O'Connors, *J. Solid State Chem.* **1991**, *94*, 362.
[10] S. Huber, C. Preitschaft, R. Weihrich, A. Pfitzner, *Z. Anorg. Allg. Chem.* **2012**, *638*, 2542.
[11] C. Pompe, A. Pfitzner, *Z. Anorg. Allg. Chem.* **2012**, *638*, 2158.
[12] A. Pfitzner, *Z. Anorg. Allg. Chem.* **1994**, *620*, 1992.
[13] A. Pfitzner, *Chem. Eur. J.* **1997**, *3*, 2032.
[14] T. Nilges, S. Reiser, J. H. Hong, E. Gaudin, A. Pfitzner, *Phys. Chem. Chem. Phys.* **2002**, *4*, 5888.
[15] M. Schur, H. Rijnberk, C. Näther, W. Bensch, *Polyhedron* **1999**, *18*, 101.
[16] K. Möller, C. Näther, A. Bannwarth, W. Bensch, *Z. Anorg. Allg. Chem.* **2007**, *633*, 2635.
[17] N. Herzberg, C. Näther, W. Bensch, *Z. Kristallogr.* **2012**, *227*, 552.
[18] B. Seidlhofer, V. Spetzler, C. Näther, W. Bensch, *J. Solid State Chem.* **2012**, *187*, 269.
[19] SCALE3 ABSPACK, *CrysAlis RED* Software, Version 171.35.21; Oxford Diffraction Ltd: Oxford, UK, **2006**.
[20] A. Altomare, M. C. Burla, M. Camalli, G. Cascarano, C. Giacovazzo, A. Guagliardi, G. Polidori, *J. Appl. Crystallogr.* **1994**, *27*, 435.
[21] G. M. Sheldrick, *SHELX 97*, Programs for Solution and Refinement of Crystal Structures, University of Göttingen, Germany, **1997**.
[22] R. D. Shannon, *Acta Crystallogr., Sect. A* **1976**, *32*, 751.
[23] V. B. Lazarev, A. V. Salov, S. I. Berul, *Russ. J. Inorg. Chem.* **1973**, *18*, 112.
[24] M. Jansen, U. Henseler, *J. Solid State Chem.* **1992**, *99*, 110.
[25] M. Pompetzki, M. Jansen, *Z. Anorg. Allg. Chem.* **2003**, *629*, 1929.
[26] T. Nilges, C. Dreher, A. Hezinger, *Solid State Sci.* **2005**, *7*, 79.
[27] W. Klemm, H. Sodomann, P. Langmesser, *Z. Anorg. Allg. Chem.* **1939**, *241*, 281.
[28] *STOE WinXPOW*, Version 1.08, STOE & Cie GmbH, Darmstadt, **2000**.
[29] *Varian Resolutions Pro*, Version 4.1.0.101, Varian, Inc., **2006**.
[30] E. Freudenthaler, A. Pfitzner, *Solid State Ionics* **1997**, *101–103*,1053.
[31] *Thales Flink*, Version 2.13; Zahner Messtechnik GmbH & Co. KG, Kronach.

Received: November 22, 2012
Published Online: February 11, 2013

